Spin-glass-like behavior in single-crystalline $Cu_{0.44}In_{0.48}Cr_{1.95}Se_4$

H. Duda,[1] E. Maciążek,[2] T. Groń,[1,*] S. Mazur,[1] A. W. Pacyna,[3] A. Waśkowska,[4] T. Mydlarz,[5] and A. Gilewski[5]
[1]*Institute of Physics, University of Silesia, ulica Uniwersytecka 4, 40-007 Katowice, Poland*
[2]*Institute of Chemistry, University of Silesia, ulica Szkolna 9, 40-006 Katowice, Poland*
[3]*The Henryk Niewodniczański Institute of Nuclear Physics, Polish Academy of Sciences, ulica Radzikowskiego 152, 31-342 Kraków, Poland*
[4]*Institute of Low Temperature and Structure Research, Polish Academy of Sciences, ulica Okólna 2, 50-950 Wrocław, Poland*
[5]*International Laboratory of High Magnetic Fields and Low Temperatures, ulica Gajowicka 95, 53-529 Wrocław, Poland*
(Received 17 August 2007; published 22 January 2008)

The complex ac dynamic magnetic susceptibility was used to study the spin-glass-like behavior in single-crystalline $Cu_{0.44}In_{0.48}Cr_{1.95}Se_4$ spinel. The broad maximum in the dc susceptibility at 44 K and the vanishing of the ac susceptibility second harmonic in the temperature range of 4.2–44 K suggest the spin-glass-like behavior. A large spin-glass-to-paramagnet transition points to the magnetically inhomogeneous state of the sample associated with nonstoichiometry. This is accompanied with the absence of the Curie-Weiss region in the temperature range of 44–360 K, which reveals also an anomaly in the second and third harmonics of the ac susceptibility. This means that the formation of spin glasses takes place also in magnetic clusters above the freezing temperature T_f=44 K. The exchange constant of the spin-glass system estimated from the random energy model equals 26.4 K. These observations are interpreted within the framework of the molecular field theory.

DOI: 10.1103/PhysRevB.77.035207 PACS number(s): 75.50.Lk, 71.20.Nr, 72.20.Pa, 75.30.Gw

I. INTRODUCTION

Much information on the physical properties of the $Cu_xIn_{1-x}Cr_2Se_4$ spinel system can be found in literature,[1–10] but so far, only the polycrystalline $Cu_{0.5}In_{0.5}Cr_2Se_4$ spinel was described in detail.[1–5] Yokoyama and Chiba reported[1] that the $Cu_{0.5}In_{0.5}Cr_2Se_4$ is a semiconductor and paramagnet above 77 K. The positive Curie-Weiss temperature, θ_{CW} =135 K, pointed to the ferromagnetic type of interactions. Later, Pinch *et al.*[2] found antiferromagnetic ordering with the Néel temperature T_N=14 K. Next, Belov *et al.*[4] discovered the spin-glass state with the freezing temperature T_f=5.8 K. The semiconducting and spin-glass behaviors were also found in the $(CuCr_2Se_4)_x(Cu_{0.5}In_{0.5}Cr_2Se_4)_{1-x}$ solid solutions in the compositional range $0 \leq x < 0.1$.[7]

Recently, magnetic investigations of the single crystals of $Cu_xIn_yCr_zSe_4$ spinel (where y=0.074, 0.1, 0.12, 0.15, 0.16, 0.48, 0.54, and 1.14) revealed a ferromagnetic ordering with the Curie temperature T_C=330 K up to y=0.16, the spin-glass-like behavior with the freezing temperature of 36 K for y=0.48, the antiferromagnetic ordering with the Néel temperature T_N=21 K for y=0.54, and, again, the ferromagnetic state appearing below T_C=290 K for y=1.14.[11] In the compositional range $0.074 \leq y \leq 0.54$, the indium ions had tetrahedral coordination, $(Cu_xIn_y)Cr_zSe_4$, while for y=1.14, the indium were octahedrally coordinated, $Cu_x[In_yCr_z]Se_4$. The $Cu_xIn_yCr_zSe_4$ spinel has a limited solubility. The parent $CuCr_2Se_4$ exhibits a strong p-type metallic ferromagnetism with the chromium spins coupled in parallel via exchange interactions involving conduction electrons.[12,13] The second end member of the system, i.e., $InCr_2Se_4$, is not known yet.[10] It was thus natural to expect a frustrated state between the ferromagnetic and antiferromagnetic phases in the $Cu_xIn_yCr_zSe_4$ system, as shown in Fig. 1. Preliminary studies[11] for the single crystal with y=0.48 pointed to the spin-glass behavior, as it was derived both from the hard magnetization process and the broad peak on the curve of the temperature dependence of magnetic susceptibility.

Therefore, the main purpose of the present work is an attempt to investigate the spin-glass-like behavior in the single crystal of the $Cu_{0.44}In_{0.48}Cr_{1.95}Se_4$ composition in more detail by applying the complex ac susceptibility, $\chi_n = \chi_n' - i\chi_n''$, measurements as a technique enabling the studies of dynamic properties of magnetic systems.[14] At low ac fields, this technique allows for reliable determination of the phase transition temperature, as it does not affect the magnetic order parameter, especially in the case of the nonlinear magnetic behavior. In the framework of this method, a pure sinusoidal field, $\boldsymbol{H}(t)=\boldsymbol{H}_{\mathrm{ac\ sin}}(\omega t)$, can induce nonsinusoidal oscillations of the magnetization which may be represented by the sum of sinusoidal components oscillating at harmonics of driving frequency ω:[15]

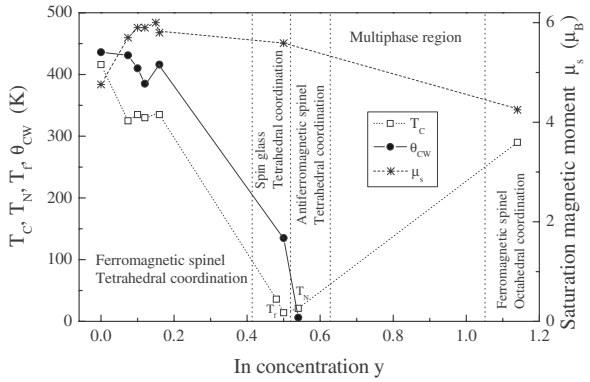

FIG. 1. Magnetic diagram for the $Cu_xIn_yCr_zSe_4$ spinel system. T_C, T_N, T_f, and θ_{CW} are the Curie, Néel, freezing, and Curie-Weiss temperatures, respectively. μ_s is the saturation magnetic moment per molecule.

$$\boldsymbol{M}(t) = \boldsymbol{H}_{\mathrm{ac}} \sum_{n=1}^{\infty} [\chi_n' \sin(n\omega t) - \chi_n'' \cos(n\omega t)], \tag{1}$$

where χ_n' and χ_n'' $(n=1,2,3,\ldots)$ are defined as the in-phase (real part) and out-of-phase (imaginary part) components of the ac susceptibility harmonics, respectively. χ_n' and χ_n'' are expressed as follows:[15]

$$\chi_n' = \frac{1}{\pi H_{\mathrm{ac}}} \int_0^{2\pi} M(t)\sin(n\omega t)d(\omega t), \tag{2}$$

$$\chi_n'' = \frac{-1}{\pi H_{\mathrm{ac}}} \int_0^{2\pi} M(t)\cos(n\omega t)d(\omega t). \tag{3}$$

For $n=1$, Eqs. (2) and (3) describe the fundamental susceptibility χ_1. Its real part χ_1' corresponds to the dispersive magnetic response and reflects a current shielding for semiconductor in this case. The imaginary part χ_1'' relates to the energy dissipation.[15] For $n>1$, there are the higher harmonics, resulting from hysteresis and nonlinearity of magnetization, which can also give valuable information on the character of the magnetic phase transitions.[14] Experimentally, the χ_n' and χ_n'' components are measured as a voltage, proportional to the time derivative of $\boldsymbol{M}(t)$, induced in a pickup coil.

II. EXPERIMENTAL PROCEDURE

A. Preparation

The single crystal of $Cu_{0.44}In_{0.48}Cr_{1.95}Se_4$ spinel was obtained by the chemical vapor transport method.[11] As the starting materials, binary selenides (CuSe and In_2Se_3) and anhydrous chromium chloride ($CrCl_3$) were used. Copper selenide (CuSe) and indium selenide (In_2Se_3) were synthesized in silicon ampoules evacuated to a pressure of about 10^{-5} Torr from elemental copper (purity of 99.999%), indium (purity of 99.99%), and selenium (purity of 99.999%). The crystal growth was carried out in a horizontal zone furnace with a melting zone temperature of 1053–1253 K and crystallization zone temperatures of 953–1101 K. The furnace was slowly cooled after 7 or 14 days of heating.

For accurate crystal structure characterization, describing the cation distribution over the tetrahedral and octahedral sites formed by the selenium sublattice, a good quality sample was selected for the intensity data collection with a single crystal x-ray diffraction technique. The intensities were measured with a KM-4/charge coupled device (Oxford Diffraction) instrument, operating in κ geometry and using graphite monochromated Mo Kα radiation ($\lambda=0.710\,73$ Å). Integration of the intensity data and corrections for Lorentz-polarization effects was made using the CRYSALIS software.[16] The absorption correction was applied with the Gaussian face-indexed numerical routine.[17] The structure calculations were performed using the SHELXL-97 program system.[17] It was considered that the In ions may occupy both the tetrahedral and octahedral sites of the spinel structure. However, the least squares structure refinement, taking into account the site occupancy factors as free parameters, has shown that the In and Cu ions are in two distinct tetrahedral positions.

The chemical composition of the $Cu_{0.44}In_{0.48}Cr_{1.95}Se_4$ single crystal was determined by the inductively coupled plasma atomic emission spectroscopy method. The measurement conditions were as follows: a frequency of 27.12 MHz, power of 1.1 kW, torch of Ar/Ar/Ar (quartz demountable), nebulizer gas of 1.01 min^{-1}, nebulizer (concentric Meinhard), nebulizer pressure of 2.4 bars, sample rate of 1.0 ml min^{-1}, observation height of 11 mm, holographic grating of 2400 grooves mm^{-1}, and dispersion of grating in first reciprocal order of 0.55 nm mm^{-1} were applied. The analytical lines (integration time) for Cr of 206.149 nm, Se of 196.026 nm, In of 325.609 nm, and Cu of 219.958 nm were used.

B. Magnetic measurements

The magnetic moment was measured in stationary fields up to 140 kOe as well as in pulsed fields up to 360 kOe at 4.2 K. Magnetization and the static (dc) and dynamic (ac) susceptibility measurements were performed using a Lake Shore 7225 ac susceptometer and/or dc magnetometer in the temperature range of 4.2–250 K as well as the Faraday-type Cahn RG automatic electrobalance in the temperature range of 4.2–360 K and in applied external magnetic field $H_{\mathrm{dc}} \approx 104$ Oe. The static dc magnetic susceptibilities were measured in two different cooling modes. In the zero-field-cooled (ZFC) mode, the sample was first cooled down in the absence of an external magnetic field and then investigated while heating in a given magnetic field. The field-cooled (FC) mode usually followed ZFC run when the same magnetic field was set on at high temperatures and measurements were performed with decreasing temperature. For both modes, the cooling process always started from the paramagnetic state.

The dynamic ac magnetic susceptibilities were measured in the ZFC mode. Before the proper ac measurements, a testing procedure was done. The in-phase $\chi'(\omega)$ and out-of-phase $\chi''(\omega)$ components of the ac susceptibility were recorded simultaneously as a function of temperature: (1) at different external static fields H_{dc} changing from 0 to 1 kOe where the internal oscillating field $H_{\mathrm{ac}}=1$ Oe with the internal frequency $f=120$ Hz was applied to a sample (Fig. 2); (2) without external static field where the internal oscillating fields H_{ac} changing from 0.1 to 10 Oe with the internal frequency $f=120$ Hz were applied to a sample (Fig. 3); and (3) without external static field where the internal oscillating field $H_{\mathrm{ac}}=1$ Oe with different internal frequencies ranging from 24 to 600 Hz was applied to a sample (Fig. 4). The zero field ac measurements were carried out by cooling a sample in a zero field from room temperature down to 4.2 K. A testing procedure described above and depicted in Figs. 2–4 shows that the increasing external static field H_{dc} damps a spin dynamics in a system from one side and a high spin dynamics both for internal frequency $f=120$ Hz and the internal oscillating field $H_{\mathrm{ac}} \geqslant 1$ Oe is observed from the other. Therefore, the signals of the first (χ_1), second (χ_2), and third (χ_3) harmonics (as defined in Sec. I) associated with nonlinear susceptibilities were detected as a function of temperature without applied external magnetic field.

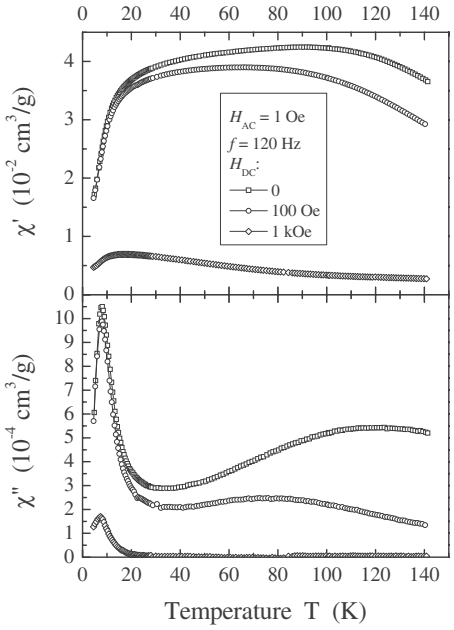

FIG. 2. Zero field susceptibilities χ' and χ'' vs temperature T at different external magnetic fields H_{dc} changing from 0 to 1 kOe where the internal oscillating field $H_{ac}=1$ Oe with internal frequency $f=120$ Hz was applied to a sample.

C. Electrical measurements

The electrical measurements have been done in the temperature range of 70–450 K. The electrical resistivity ρ has been measured with the aid of the four-point dc method using the HP 34401A digital multimeters. The maximal error $\delta\rho/\rho$ was less than $\pm 1\%$. The thermoelectric power was measured with a differential method using the temperature gradient ΔT of about 5 K. The accuracy of the value of thermopower was estimated to be better than 3 μV/K.

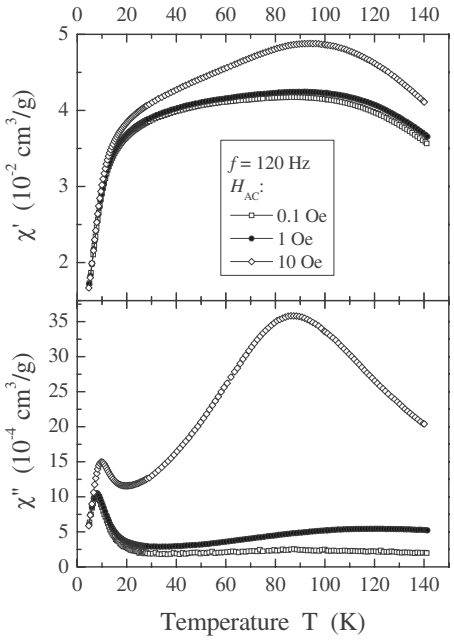

FIG. 3. Zero field susceptibilities χ' and χ'' vs temperature T at different internal oscillating magnetic fields H_{ac} changing from 0.1 to 10 Oe with internal frequency $f=120$ Hz (the external magnetic field $H_{dc}=0$ Oe).

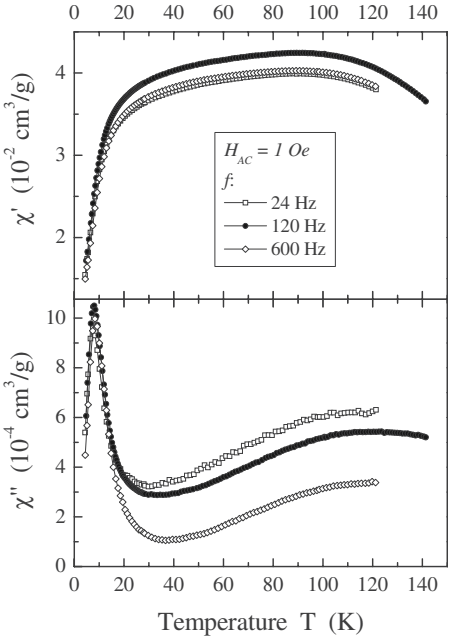

FIG. 4. Zero field susceptibilities χ' and χ'' vs temperature T at different internal frequencies f ranging from 24 to 600 Hz with oscillating field $H_{ac}=1$ Oe (the external magnetic field $H_{dc}=0$ Oe).

III. RESULTS

A. Crystallographic properties

Crystal data, experimental details, and structure refinement results for single-crystalline $Cu_{0.44}In_{0.48}Cr_{1.95}Se_4$ spinel are collected in Table I. They have shown that the compound crystallizes in the cubic structure with space group $F\bar{4}3m$ (No. 216) and the unit cell of dimension $a=1057.35$ pm, being elongated in comparison with $a=1033.5(3)$ pm of the parent $CuCrSe_4$.[13] Two diamagnetic ions, Cu and In, differing in ionic radii and charge ($r_{Cu}+=60$ and $r_{In3+}=63$ pm),[18] occupy two distinct tetrahedral 4a and 4d positions, respectively, while the magnetic Cr ions are in the octahedral 16e sites. Refinement of the site occupation factors (SOFs) revealed a certain amount of the cation deficit in both tetrahedral A sites (Table I). Such cation distribution causes the presence of two types of tetrahedra with the A-to-selenium distances of 243.4(1) and 253.7(1) pm for Cu and In, respectively. This entails distortion of the octahedra built about the Cr^{3+} ions (Table I). The local features arising from the subtle misfit of the polyhedra together with the cation deficit give rise to the formation of the structural clusters of different sizes and cation concentrations. These effects have strong impact on magnetic properties of the sample under study.

B. Electrical properties

The electrical resistivity measurement reveals a semiconducting behavior of the Arrhenius type with two cusps at 117

TABLE I. Crystal data, experimental details, and structure refinement results for the $Cu_{0.44}In_{0.48}Cr_{1.95}Se_4$ single crystal.

(I) Crystal data				
Crystal system, space group		Cubic, $F\bar{4}3m$		
Unit cell dimension a (pm)		1057.35(9)		
Volume (m^3)		1.18211×10^{-27}		
Calculated density d (Mg/m^3)		8.5792		
Crystal size ($mm\times mm\times mm$)		$0.1\times0.1\times0.09$		
(II) Data collection				
Wavelength (Å)		0.71073		
2θ maximum for data collection (deg)		92.25		
Limiting indices: h		−18, 21		
k		−21, 12		
l		−13, 21		
Reflections collected		5706		
Reflections unique		573		
Reflections $>2\sigma(I)$		459		
Absorption coefficient (mm^{-1})		31.85		
Absorption correction		Numerical		
R(int) before, after abs. correction		0.098, 0.055		
(III) Refinement				
Refinement method		Full-matrix least squares on F^2		
Number of refined parameters		15		
Goodness of fit on F^2		1.020		
Final R indices $[I>2\sigma(I)]$: R_1		0.040		
wR_2		0.099		
Largest diff. peak and hole (e Å^{-3})		2.18 and −1.49		
(IV) Atomic positions				
Atom	Site	Wyckoff position	SOF	U_{iso}[a] (10^3 Å^2)
Cu	A	4a (0, 0, 0)	0.88	1.55(6)
In	A	4d $(\frac{3}{4},\frac{3}{4},\frac{3}{4})$	0.99	1.68(3)
Cr	B	16e [0.6292(1)]	0.975	1.70(2)
Se(1)	X	16e [0.61149(5)]	1.0	1.67(2)
Se(2)	X	16e [0.13295(5)]	1.0	1.50(2)
(V) Selected interatomic distances and angles				
Cu-Se(2) (pm)		243.42(10)		
In-Se(1) (pm)		253.69(10)		
Cr-Se(1) (pm)		255.98(13)		
Cr-Se(2) (pm)		251.47(10)		
Se(2)-Cu/In-Se(2) (deg)		109.47(0)		
Se(2)-Cr-Se(2) (deg)		88.25(7)		
Se(1)-Cr-Se(2) (deg)		95.16(2)		
Se(2)-Cr-Se(1) (deg)		175.25(9)		
Se(1)-Cr-Se(1) (deg)		81.26(7)		

[a]U_{iso} is the isotropic displacement parameter.

and 253 K (Fig. 5). As shown in Fig. 6, the temperature dependence of thermoelectric power is more complex. First, a change of the sign of the thermopower from negative to positive takes place at 80 K, and then a small positive cusp appears at 110 K, followed by a broad plateau close to 0 μV/K in the temperature range of 170–330 K, and finally, a sharp increase in thermopower above 350 K can be observed. The dotted line in Fig. 6 suggests that the diffusion

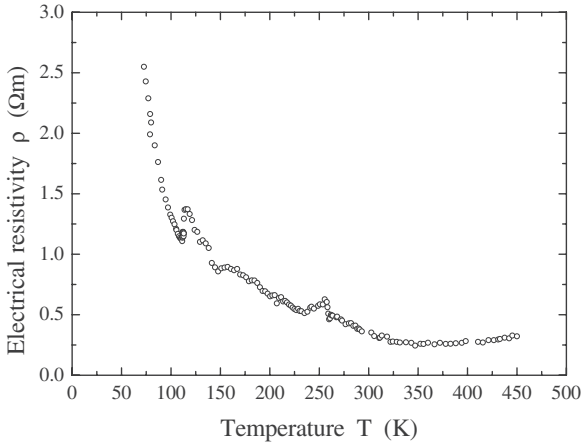

FIG. 5. Electrical resistivity ρ vs temperature T.

processes in the electronic transport dominate at higher temperatures, well above 420 K. On the other hand, at lower temperatures, a strong competition between impurity, phonon drag, and magnon drag components of thermopower coming both from electrons and holes takes place.

C. Magnetic properties

The results of the magnetic measurements are depicted in Figs. 7–12. The magnetic isotherms (Fig. 7), taken at 4.2 K and in magnetic stationary (up to 140 kOe) and in pulsed (up to 360 kOe) fields H, indicate that $Cu_{0.44}In_{0.48}Cr_{1.95}Se_4$ exhibits hard magnetization and the magnetic moment reaches the value close to $5.73\mu_B$ per molecule in the magnetic fields $H=360$ kOe. This means that the chromium Cr^{3+} ions occupy the octahedral sites alone and they are in the high spin configuration of the $3dt_{2g}$ orbital. These results correlate well with the crystallographic data (Table I). By comparing with the parent $CuCr_2Se_4$ spinel showing easy magnetization,[12] we suggest that the structure distortion resulting from substitution of the In for Cu ions in the tetrahedral sites leads to the hard magnetization and the complex magnetic structures result from frustration of the magnetic moments. The shape of the temperature dependence of the magnetization curve measured in the magnetic induction $B=0.5$ T (Fig. 8) points to

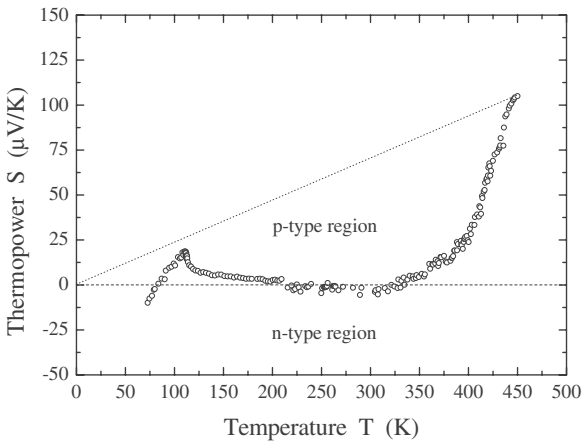

FIG. 6. Thermoelectric power S vs temperature T.

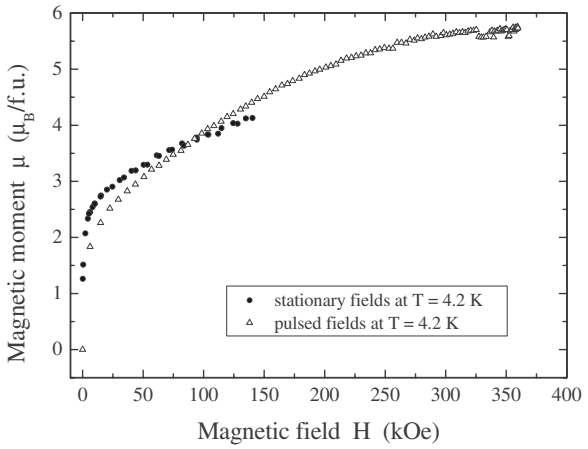

FIG. 7. Magnetic moment μ versus stationary and pulsed magnetic field H measured at 4.2 K.

the disorder magnetic structure. This corroborates the magnetic dc susceptibility data. The broad maximum in the ZFC mass susceptibility close to 44 K measured in the stationary field $H_{dc}=104$ Oe (Fig. 9) suggests the spin-glass-like behavior. This observation is confirmed both by the ZFC and FC temperature measurements of susceptibility in the stationary field $H_{dc}=100$ Oe (Fig. 10) and the absence of the Curie-Weiss region in the temperature range of 44–360 K (Fig. 9). A transition to the paramagnetic region is expected and we also measure the susceptibility at higher temperatures.

The temperature dependences of the zero field in-phase $\chi_1'(T)$ (real part) and out-of-phase $\chi_1''(T)$ (imaginary part) components of fundamental susceptibility measured at the oscillating field $H_{ac}=1$ Oe and at the constant frequency of 120 Hz are depicted in Fig. 11. The broad maximum at 60 K in the real part of the ac measurement $\chi_1'(T)$ coincides well with the broad maximum observed in the dc measurement. The imaginary part of the ac susceptibility $\chi_1''(T)$ shows a sharp peak at 10 K with large intensity, a broad minimum at 36 K, and a broad maximum at 137 K. Such a type of maxima in the $\chi_1''(T)$ dependences are usually associated with the energy losses, connected, for example, with the

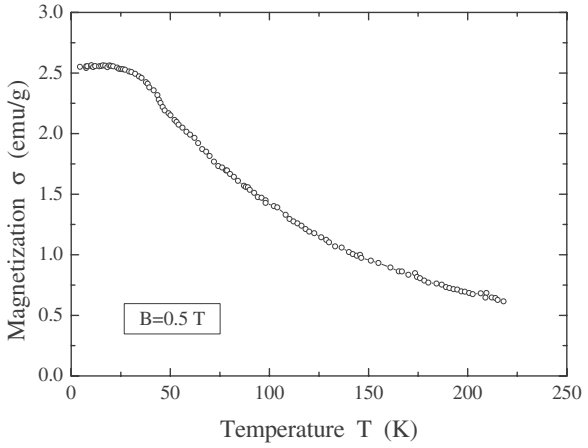

FIG. 8. Zero field cooled dc mass magnetization σ vs temperature T measured in magnetic induction $B=0.5$ T.

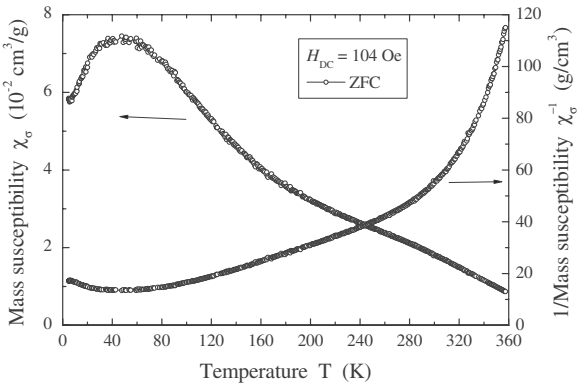

FIG. 9. Temperature dependences of zero-field-cooled dc mass susceptibility χ_σ and reciprocal mass susceptibility χ_σ^{-1} recorded at H_{dc}=104 Oe.

magnetic-domain-wall motion or with rotation of magnetization within domains.[19] A characteristic minimum in the $\chi_1''(T)$ dependence may indicate a frozen spin state. Higher harmonic susceptibilities (χ_2 and χ_3), described theoretically by Eqs. (2) and (3), were measured in the temperature range of 4.2–250 K and at the oscillating field H_{ac}=5 Oe and at the constant frequency f=120 Hz (Fig. 12). The zero field in-phase and out-of-phase second harmonics of susceptibilities $\chi_2'(T)$ and $\chi_2''(T)$ vanish in the temperature range of 4.2–44 K. The second harmonic $\chi_2'(T)$ becomes negative and $\chi_2''(T)$ is positive above 44 K. Their temperature dependences have almost asymmetrical shape. Each of the second harmonics shows two extremes: $\chi_2'(T)$ at 142 and 200 K and $\chi_2''(T)$ at 151 and 216 K. The third harmonic appears to be more complicated. Its real part $\chi_3'(T)$ changes sign from negative to positive at 100 K and exhibits two positive maxima at 141 and 222 K. The imaginary part $\chi_3''(T)$ is positive and reveals a huge maximum at 116 K. An anomalous shape of the second and third harmonics described above may indicate the spin-glass state in the magnetic clusters, especially in the temperature range where the Curie-Weiss region does not occur.

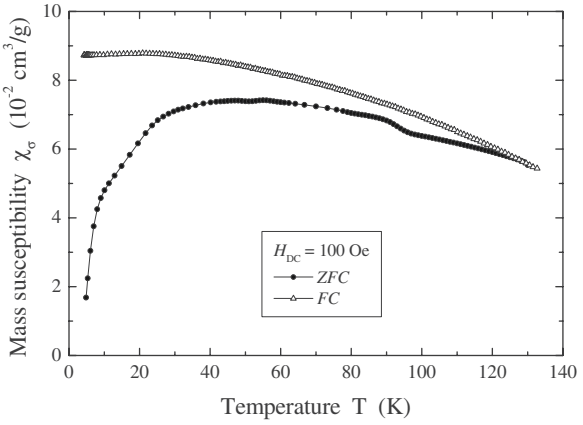

FIG. 10. Temperature dependence of ZFC and FC dc mass susceptibilities χ_σ recorded at H_{dc}=100 Oe.

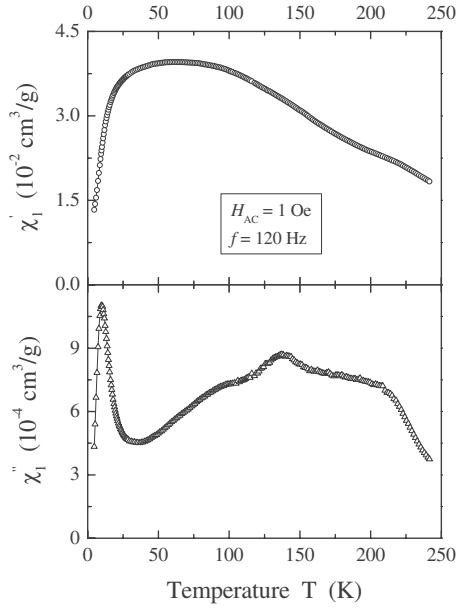

FIG. 11. Zero field susceptibilities $\chi_1'(T)$ and $\chi_1''(T)$ recorded simultaneously as a function of temperature T with internal frequency f=120 Hz at oscillating field H_{ac}=1 Oe.

IV. DISCUSSION

The present electrical and magnetic results do not show a clear order-disorder phase transition in the temperature range of 4.2–450 K in the classical meaning in the single-crystalline $Cu_{0.44}In_{0.48}Cr_{1.95}Se_4$ spinel. The broad peak close to 44 K in the ZFC dc and ac susceptibility curves suggests the spin-glass-like magnetic structure. Next, the difference between ZFC and FC susceptibilities persisting above the freezing temperature up to 130 K is indicative of the mag-

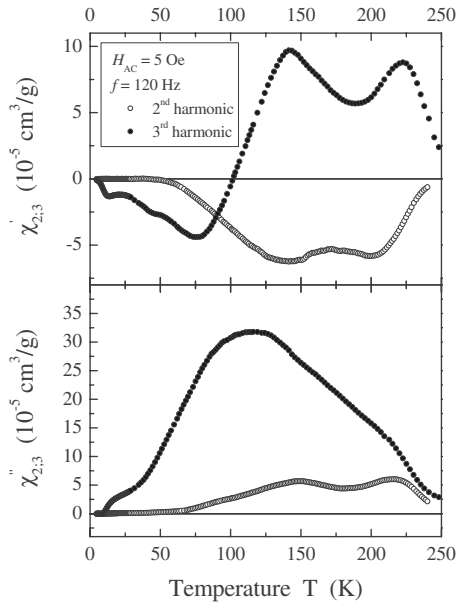

FIG. 12. Temperature dependence of the real and imaginary components of zero field susceptibilities (second and third harmonics $\chi_{2;3}'$ and $\chi_{2;3}''$) with internal frequency f=120 Hz at oscillating field H_{ac}=5 Oe.

netic cluster spin-glass structure. Such behavior is related to nonstoichiometry, lack of the Curie-Weiss temperature region, and hard magnetization of the sample. It also finds reflection in the lower cubic symmetry $F\bar{4}3m$ of the single-crystalline $Cu_{0.44}In_{0.48}Cr_{1.95}Se_4$ spinel in which the structural clusters are formed because the location of In and Cu ions in two distinct tetrahedral sites causes a mishmash of the A-Se and Cr-Se chemical bonds to grow longer by about a few picometers in comparison with the corresponding bonds in $CuCr_2Se_4$ spinel having high cubic symmetry $Fd3m$.[13] As a consequence, the transition range between quasiordered spin-glass state and disordered paramagnetic state (if it exists) is very large; it can exceed the freezing temperature by several times indicating, eventually, the existence of frustrated spin state.

The temperature of order-disorder phase transition is typically determined at the inflection point of the temperature dependence of dc magnetization especially in the case when a clear cusp in dc susceptibility curve is not observed. For $Cu_{0.44}In_{0.48}Cr_{1.95}Se_4$, the freezing temperature between the spin-glass-like and the paramagnetic states was shown to be T_f=44 K. This temperature is close to that obtained from the ac susceptibility measurements. For example, the imaginary part of the ac susceptibility $\chi_1''(T)$ shows the minimum at 36 K (Fig. 11). This means that in the frozen spin state, energy is not dissipated. Thus, the method of minimum in the imaginary part of fundamental susceptibility could be a good tool for determining the freezing temperature T_f. On the other hand, in the framework of molecular field theory, it was shown that the second harmonic should vanish at the temperature of magnetic ordering.[20] In our case, both real $\chi_2'(T)$ and imaginary $\chi_2''(T)$ parts of the second harmonic of susceptibility $\chi_2(T)$ vanish at 44 K. Above this temperature, where the absence of the Curie-Weiss region is observed, the two harmonics $\chi_2'(T)$ and $\chi_2''(T)$ show nonvanishing asymmetrical behavior. A similar behavior of the second harmonic of the dynamic magnetic susceptibility was observed in the single crystal of $CuCr_{1.7}Sb_{0.3}S_4$ spinel with freezing temperature T_f=47.4 K.[21,22] Additionally, the nonzero values of the χ_2 and χ_3 harmonic components above 44 K prove directly the existence of the spontaneous magnetic moments.

By knowing the freezing temperature T_f from experiment, we can estimate the exchange constant J of the spin-glass system using the random energy model[23–25] including N interacting spins with infinite-ranged random p-spin couplings. For such a model, the Hamiltonian is[25]

$$H = -\sum_{i_1 \cdots i_p} J_{i_1 \cdots i_p} S_{i_1} \cdots S_{i_p}, \tag{4}$$

where the S_i are the Ising spins, and the sum is over all groups of p spins in the system. The interactions have Gaussian distribution suitably scaled with N and p to obtain a sensible limit as N and p tend to infinity. As a result, the free energy F is temperature independent for $T \leqslant T_f$, and for $T > T_f$, it changes with temperature as follows:[23]

$$F = -N\left(T \ln 2 + \frac{J^2}{4T}\right). \tag{5}$$

This random energy model has a critical temperature known as the freezing temperature T_f, which reads as[23]

$$T_f = \frac{J}{(4 \ln 2)^{1/2}}. \tag{6}$$

Below T_f, the system is frozen in its ground state and both the specific heat and entropy vanish in the whole low-temperature phase. A similar behavior of these quantities is predicted by the mean-field theory for ferromagnetic systems.

For the $Cu_{0.44}In_{0.48}Cr_{1.95}Se_4$ single crystal, the freezing temperature T_f=44 K and, thus, the exchange constant of the spin-glass system calculated from Eq. (6) is J=26.4 K. For comparison, the exchange constant for the $CuCr_2Se_4$ p-type ferromagnetic conductor equals 171.5 K.[26] This means that the magnetic coupling in the spin-glass state of the single crystal under study is over six times weaker than that in the ferromagnetic phase.

In conclusion, the complex ac dynamic magnetic susceptibility data are a sensitive tool for the spin-glass system studies as well as for determining the freezing temperature. The vanishing of the second harmonic appears to be a method suitable for controlling the temperature region of the spin-glass state. For the single crystal under study, the second harmonic of the dynamic magnetic susceptibility takes the value close to zero in the temperature range of 4.2–44 K.

ACKNOWLEDGMENTS

This work was partly supported by the Ministry of Science (Poland).

*Corresponding author: tadeusz.gron@us.edu.pl

[1] H. Yokoyama and S. Chiba, J. Phys. Soc. Jpn. **27**, 505 (1969).
[2] H. L. Pinch, M. J. Woods, and E. Lopatin, Mater. Res. Bull. **5**, 425 (1970).
[3] C. Wilkinson, B. M. Knapp, and J. B. Forsyth, J. Phys. C **9**, 4021 (1976).
[4] K. P. Belov, L. I. Koroleva, A. I. Kuzminykh, and S. I. Usanin, Solid State Phys. **24**, 1298 (1982).
[5] A. I. Abramovich, T. V. Virovets, and L. I. Koroleva, Zh. Eksp. Teor. Fiz. **96**, 1066 (1989).
[6] R. Plumier and M. Sougi, Solid State Commun. **69**, 341 (1989).
[7] L. I. Koroleva and T. V. Virovets, Phys. Status Solidi B **157**, 431 (1990).
[8] I. Okońska-Kozłowska and I. Jendrzejewska, J. Alloys Compd. **215**, 157 (1994).
[9] T. I. Koneshova, Inorg. Mater. **28**, 928 (1992).
[10] I. Okońska-Kozłowska, E. Maciążek, K. Wokulska, and J. Heimann, J. Alloys Compd. **219**, 97 (1995).
[11] E. Maciążek, H. Duda, T. Groń, T. Mydlarz, and A. Kita, J. Alloys Compd. **442**, 183 (2007).

[12] F. K. Lotgering, in *Proceedings of the International Conference on Magnetism, Nottingham, 1964* (Institute of Physics, London, 1965), p. 533.
[13] F. K. Lotgering and R. P. Van Stapele, Solid State Commun. **5**, 143 (1967).
[14] K. Łątka, R. Kmieć, A. W. Pacyna, R. Mishra, and R. Pöttgen, Solid State Sci. **3**, 545 (2001).
[15] T. Ishida and R. B. Goldfarb, Phys. Rev. B **41**, 8937 (1990).
[16] CRYSALIS CCD and CRYSALIS RED, Oxford Diffraction Ltd., 2004, Wrocław, Poland.
[17] G. M. Sheldrick, SHELXL-99, program for the refinement of crystal structures, University of Göttingen, 1997.
[18] R. D. Shannon, Acta Crystallogr., Sect. A: Cryst. Phys., Diffr., Theor. Gen. Crystallogr. **32**, 751 (1976).
[19] T. Sato, T. Ando, T. Watanabe, S. Itoh, Y. Endoh, and M. Furusaka, Phys. Rev. B **48**, 6074 (1993).
[20] T. Hashimoto, A. Sato, and Y. Fujiwara, J. Phys. Soc. Jpn. **35**, 81 (1973).
[21] J. Krok-Kowalski, J. Warczewski, P. Gusin, P. Liszkowski, K. Krajewski, L. I. Koroleva, A. Pacyna, T. Mydlarz, and S. Matyjasik, J. Magn. Magn. Mater. **242**, 921 (2002).
[22] G. A. Govor, T. Groń, F. A. Khan, J. Krok-Kowalski, I. V. Medvedeva, I. O. Troyanchuk, and C. P. Yang, in *Double Exchange in Heusler Alloys and Related Materials*, edited by M. Annaorazov and K. Bärner (Research Signpost, Trivandrum, 2007), p. 158.
[23] B. Derrida, Phys. Rev. Lett. **45**, 79 (1980).
[24] B. Derrida, Phys. Rev. B **24**, 2613 (1981).
[25] K. Binder and A. P. Young, Rev. Mod. Phys. **58**, 801 (1986).
[26] J. Krok, J. Spałek, S. Juszczyk, and J. Warczewski, Phys. Rev. B **28**, 6499 (1983).